Nitrous oxide emissions in the Shanghai river network: implications for the effects of urban sewage and IPCC methodology

ZHONGJIE YU, HUANGUANG DENG, DONGQI WANG, MINGWU YE, YONGJIE TAN, YANGJIE LI, ZHENLOU CHEN and SHIYUAN XU

Department of Geography, School of Resources and Environment Science, East China Normal University, Shanghai 200062, China

Abstract

Global nitrogen (N) enrichment has resulted in increased nitrous oxide (N_2O) emission that greatly contributes to climate change and stratospheric ozone destruction, but little is known about the N_2O emissions from urban river networks receiving anthropogenic N inputs. We examined N_2O saturation and emission in the Shanghai city river network, covering 6300 km^2, over 27 months. The overall mean saturation and emission from 87 locations was 770% and 1.91 mg N_2O-N m^{-2} d^{-1}, respectively. Nitrous oxide (N_2O) saturation did not exhibit a clear seasonality, but the temporal pattern was co-regulated by both water temperature and N loadings. Rivers draining through urban and suburban areas receiving more sewage N inputs had higher N_2O saturation and emission than those in rural areas. Regression analysis indicated that water ammonium (NH_4^+) and dissolved oxygen (DO) level had great control on N_2O production and were better predictors of N_2O emission in urban watershed. About 0.29 Gg N_2O-N yr^{-1} N_2O was emitted from the Shanghai river network annually, which was about 131% of IPCC's prediction using default emission values. Given the rapid progress of global urbanization, more study efforts, particularly on nitrification and its N_2O yielding, are needed to better quantify the role of urban rivers in global riverine N_2O emission.

Keywords: IPCC method, land use, nitrous oxide, river network, urban sewage

Received 27 March 2013 and accepted 26 May 2013

Introduction

Over the past few decades, human activities, particularly the use of synthetic fertilizers in agriculture, have severely impacted the balance of nitrogen (N) biogeochemical cycles, causing unintended environmental issues on both regional and global scales (Davidson, 2009). Enrichment of bioactive N in terrestrial and aquatic ecosystems leads to increased emissions of nitrous oxide (N_2O), a long-lived potent greenhouse gas and ozone-depleting substance, greatly contributing to future climate change (Ravishankara *et al.*, 2009). N_2O emission from global river systems is currently estimated to be 0.9 Tg yr^{-1}, or about 17% of anthropogenic agricultural N_2O emissions, by assuming a linear relationship between dissolved inorganic nitrogen (DIN) inputs to rivers and riverine N_2O emissions (Rosamond *et al.*, 2012). However, recent studies showed that riverine N_2O emission is the most uncertain component of this current estimate of river systems due to a combination of insufficient data set and poor understanding regarding the mechanisms controlling riverine N_2O dynamics spatially and temporally (Ivens *et al.*, 2011).

N_2O production in streams and rivers are a function of rates of both nitrification and denitrification (Beaulieu *et al.*, 2010a). Consequently, the methodology of Intergovernmental Panel on Climate Change (IPCC) tabulates riverine N_2O emissions by using emission factors derived from N_2O yields of these processes, (N_2O: nitrogen gas (N_2) and N_2O: nitrate (NO_3^-) respectively), that is, $EF_{5\text{-}r}$ for N leaching and runoff, and $EF_{EFFLUENT}$ for human consumption of crops followed by municipal sewage treatment. As supported by numerous studies, NO_3^- is the dominant N form in surface water draining agricultural land and serves as the best predictor of N_2O emission generated from leaching N loads to large rivers (Clough *et al.*, 2007; Yan *et al.*, 2012). The empirical relationship between N_2O flux and NO_3^- concentration has been validated across a variety of river systems primarily due to the well-understood denitrification rate (Baulch *et al.*, 2011). However, field measurements indicated that the

Present address: Zhongjie Yu, Department of Earth and Environmental Sciences, Rutgers University, Newark, NJ 07102, USA

Correspondence: Dongqi Wang, tel. +86-21-54341201, fax +86-21-54341201, e-mail: dqwang@geo.ecnu.edu.cn

value of EF$_{5-r}$, 0.25% of total leaching N to rivers (De Klein *et al.*, 2006), could still be either overestimated or underestimated (Table S1), largely depending on the presence of N$_2$O hotspots and/or the magnitude of N$_2$O yields. EF$_{EFFLUENT}$ given by IPCC is 0.5% of the total sewage N effluent released to rivers (Doorn *et al.*, 2006) and has not been carefully examined. Only one previous study of riverine N$_2$O emission took both EF$_{5-r}$ and EF$_{EFFLUENT}$ into account (Rosamond *et al.*, 2012).

Thus, another potential reason for the large uncertainties in the current N$_2$O budget is that simple emission factors may not hold across all rivers that vary markedly in terms of N source and N$_2$O yield, which are influenced effectively by land use and intensity of human activities in watersheds (Outram & Hiscock, 2012). There are disproportionately high N$_2$O emission from rivers draining urban areas, where the relationship between NO$_3^-$ and N$_2$O flux was obscured (Rosamond *et al.*, 2012). Riverine nitrification and denitrification rates are sensitive to land use due to its varying substrates delivery (Toyoda *et al.*, 2009; Beaulieu *et al.*, 2010a); hotspots of N$_2$O emission within basins can be caused by direct N$_2$O input from wastewater treatment plant (WWTP) effluents and/or higher rates of *in situ* N$_2$O production (Hemond & Duran, 1989; Cébron *et al.*, 2005). Our preliminary study in Shanghai, China has shown the short-term N$_2$O emission from NH$_4^+$-enriched rivers is greater than the highest published emission rate (Wang *et al.*, 2009), highlighting the ability of polluted small urban rivers in removing anthropogenic N inputs (Wollheim *et al.*, 2008). Yet, N$_2$O dynamics in urban river systems are not as well studied as in agricultural systems and N$_2$O emissions from the highly urban-impacted sections cannot be explicitly resolved by process-oriented N models using basin-averaged inputs and exports (Ivens *et al.*, 2011). Nor is the role of NH$_4^+$, a good indicator of domestic pollution and sewage loads, strongly linked to *in situ* N$_2$O production, despite the assumption in the IPCC method that nitrification rates in rivers exceed denitrification by twofold. Given the estimates that N input to rivers via urban sewage will continue to increase globally (Van Drecht *et al.*, 2009), associated with faster rate of urbanization particularly in developing countries and areas (Seto *et al.*, 2012), it is a pressing need to better quantify and understand N$_2$O emissions from urban rivers to constrain the estimate of this atmospheric N$_2$O burden.

In this study, we report a 27-month, basin-wide investigation on N$_2$O saturation and emission in the highly urbanized Shanghai river network. Annual N input through leaching and sewage to the river network was also compiled from varying land uses. We use these data to examine controls on N$_2$O production in urban rivers, estimate annual N$_2$O emission from the whole river network, and examine the IPCC methodology to assess global riverine N$_2$O emission.

Materials and methods

Site description and land use

Shanghai, one of the most populated metropolises in the world (more than 23 million people), sits on the coast of the East China Sea and the Yangtze River Delta. In this area, the river network is dense, with over 1000 rivers and river length totaling >1500 km (Xu, 2004). The total water area of the river network is 569.6 km^2, equivalent to about 9% of Shanghai's total terrain (6300 km^2). Together with its main tributaries, Suzhou Creek, Wenzaobang Creek and Dianpu River, the Huangpu River system provides over 80% of Shanghai's water supply and constitutes the backbone of the river network. The hydrological parameters, including water level, water velocity, and discharge, of the rivers span a broad range depending largely on tidal motion, dam control, and river order. The annual mean water velocity and discharge of Huangpu River are 0.8 m s^{-1} and 400 m^3 s^{-1}, respectively (Shanghai Water Bureau, 2011).

We loaded ETM+ images onto the Landsat7 software and generated the river surface area, river length, and land use map by employing ESRI ARCGIS 9.2 software. This study divides Shanghai into three kinds of areas, urban, suburban, and rural, according to urban (the sum of commercial areas, public facilities, and urban residences), industrial, and agricultural land portions in ten administrative districts (Table 1). Urban areas (SP, MH, BS, JD) are characterized by dominant urban and industrial land use; districts in suburban areas (PD, SJ, JS, QP, FX) serve multiple municipal functions, including considerable agricultural land (≥45%) and minor portions of urban and industrial usage; CM, separated from mainland Shanghai by Yangtze River, is the farthermost rural area.

We set 4 to 15 sampling sites in each administrative district, depending on the river length, river density and river order, which result in 87 sampling sites in total covering all primary rivers in Shanghai area from its headwater catchment to the mouth that connects the Yangtze Estuary (Fig. 1). The width of selected sampling rivers ranges from 9 to 531 m, representative of the whole river network. The depth of low-order rivers we sampled was measured to be 0.8–2.5 m, while the depth of sampled high-order rivers, like Huangpu River and its main tributaries, was reported to be 6–10 m (Shanghai Water Bureau, 2011).

Sample collection and analysis

This study consists of 13 sampling campaigns and spans a 27-month period. The first two sampling campaigns were conducted in August and December of 2009, respectively. Eleven sampling sites in CM (rural rivers) were not sampled in these two campaigns. From February 2010 through October 2011 the remaining 11 sampling campaigns were conducted bimonthly at all 87 sites. We collected water samples for dissolved N$_2$O analysis using a headspace equilibration technique. Briefly,

Table 1 Land use classification, number of WWTPs, and chemical characteristics of river water in study sites[*]

	District	Land use (%) Urban	Industry	Agriculture	Total river length (km)[†]	DO (mg l^{-1})	NH$_4^+$-N (mg l^{-1})	NO$_3^-$-N (mg l^{-1})	DIC (mg l^{-1})	DOC (mg l^{-1})	SO$_4^{2-}$ (mg l^{-1})
Urban area	SP	68	16	1	258	3.21 (nd–12.0)	5.40 (0.34–19.7)	3.64 (0.14–12.9)	31.9 (19.4–85.1)	31.6 (7.83–245.5)	119.5 (48.7–150.2)
	MH	31	23	33	1546	3.51 (0.12–9.33)	3.04 (0.08–18.2)	3.90 (0.96–11.0)	26.2 (16.7–40.5)	22.6 (7.67–49.2)	108.4 (33.2–173.8)
	BS	27	23	39	2291	2.83 (nd–8.41)	5.76 (0.81–20.6)	3.49 (0.09–13.9)	32.2 (22.6–42.7)	28.0 (6.66–52.6)	96.6 (53.1–142.6)
	JD	24	18	44	1870	3.64 (nd–8.62)	3.80 (0.22–15.8)	4.28 (0.32–37.8)	29.7 (17.6–39.4)	26.0 (4.91–53.8)	106.5 (37.1–193.7)
Suburban area	PD	28	14	45	2276	4.68 (0.76–15.9)	2.50 (0.11–9.49)	3.53 (0.63–14.0)	32.4 (15.2–62.5)	22.5 (5.05–60.1)	83.8 (39.9–201.4)
	SJ	19	12	54	1939	4.61 (0.75–10.2)	2.31 (0.17–10.2)	4.50 (0.62–21.8)	23.7 (8.01–38.1)	21.4 (6.93–49.8)	91.9 (41.9–162.2)
	JS	17	6	66	2610	4.10 (0.26–8.70)	2.20 (0.54–8.50)	3.97 (0.48–19.2)	28.7 (21.4–36.9)	24.5 (8.80–49.4)	96.7 (46.6–130.4)
	QP	14	8	53	2127	4.48 (0.13–12.2)	2.84 (0.14–13.7)	4.65 (0.35–31.5)	25.4 (12.3–44.3)	26.4 (8.36–53.5)	111.3 (52.0–182.9)
	FX	10	12	64	1649	4.53 (0.12–12.0)	2.19 (0.23–11.9)	4.78 (0.47–19.2)	26.2 (15.6–36.0)	23.7 (6.24–49.9)	96.7 (40.7–123.9)
Rural area	CM	12	1	80	2027	6.14 (1.64–11.9)	1.25 (0.14–11.1)	1.69 (0.41–4.9)	29.1 (18.0–55.5)	31.5 (4.63–93.3)	62.9 (37.7–206.5)

*If the water chemistry data are log normally distributed rather than normally distributed, the population mean is computed; 'nd' means not detected.
†River length data is from Xu et al. (2004).

during each sampling visit, triplicate samples of surface river water (ca. 10 cm depth) were collected from cross-river bridges using an air-tight water sampler and then extruded directly into a 140-ml gas-tight sampling tube, which was fully filled and immediately sealed without any air bubbles being contained. Meanwhile, two 180-ml atmospheric gas samples were collected and injected into pre-vacuumed gas bags using syringe equipped with three-way valve. *In situ* water temperature, pH, salinity, and dissolved oxygen (DO) of surface water and air temperature were measured by calibrated portable instruments. One hundred and fifty milliliter of surface water was collected and stored in a plastic bottle for NH$_4^+$ and NO$_3^-$ measurement in all campaigns except June 2011 (due to an instrument failure in the laboratory). In addition, 150 ml of surface water was collected for the measurement of dissolved inorganic carbon (DIC), dissolved organic carbon (DOC), and sulfate (SO$_4^{2-}$) in six sampling campaigns from February 2010 through December 2010 for all sampling sites. All samples were obtained during daytime, and water samples were stored under ice and processed in the laboratory within 6 h. Each water sample for gas analysis was preserved with 0.2 ml saturated mercuric chloride solution at 4 °C until analysis (within 7 days).

For N$_2$O concentration measurement, a headspace was created by injecting 60 ml ultra-pure N$_2$ through the top septum of the sampling tube, while a needle penetrating into the bottom septum allowed an equal volume of water to escape. The sampling tube was then shaken vigorously for 5 min to let gas diffuse out and N$_2$O to equilibrate between the headspace and water phase. Ten milliliter of the headspace gas, and 30 ml from gas bag in the case of atmospheric N$_2$O measurement, was drawn out and injected into a gas chromatograph.

N$_2$O concentration was determined using a gas chromatograph with electron capture detection, two Poropak Q columns for analysis and backflush (1 m × 2 mm and 3 m × 2 mm, respectively), and a 1-ml sample loop. A 95 : 5 mixture of Ar/CH$_4$ was used as the carrier gas flowing at 35 cm^3 min^{-1} through the column. The system was single-point calibrated with 347.7 ppbv N$_2$O standard after measuring every six consecutive samples. System precision was less than 1% relative standard deviation at approximately ambient concentrations.

Dissolved NH$_4^+$ was analyzed using Nessler's reagent spectrophotometry. Dissolved NO$_3^-$ and SO$_4^{2-}$ were measured using automated colorimetry. DIC and DOC were measured using a TOC analyzer with high-temperature Pt-catalyzed combustion and NDIR detection.

Data calculation and statistical test

Concentrations of dissolved N$_2$O in the river water samples were calculated with the appropriate Bunsen coefficient (Wang *et al.*, 2009). N$_2$O equilibrium concentrations in the river water were determined using the ambient atmospheric N$_2$O partial pressure and the temperature-dependent solubility coefficient for N$_2$O given by Weiss & Price (1980). Dissolved N$_2$O concentrations were then expressed in terms of percentage saturation based on the N$_2$O equilibrium concentration. We estimated gas emission rate using the two-layer
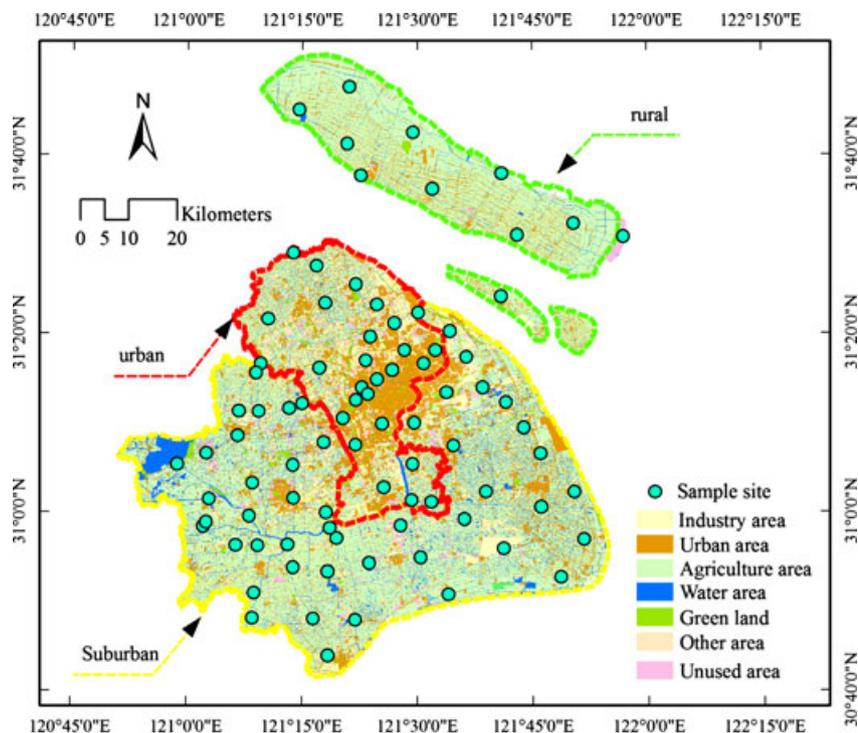
Fig. 1 Location of sampling sites and its corresponding land use.

model of diffusive gas exchange. Eqn (1) was used to model a predictive emission rate:

$$F = k \times (C_w - C_a), \tag{1}$$

where F is the gas flux, and positive number means net N_2O emission; C_w is measured N_2O concentration in the river water; C_a is measured N_2O concentration in ambient air of the sampling river; k is the transfer coefficient standing for the water turbulence. In this study, k was calculated from a wind-dependent model derived from field floating-dome, natural tracer, and tracer addition measurements specifically for estuarine rivers (Raymond & Cole, 2001):

$$k = 1.91e^{0.35\mu}(Sc/600)^{-1/2} \tag{2}$$

where Sc is the Schmidt number for N_2O corrected by *in situ* water temperature; μ is long-term wind speed at 10 m height above the river. To precisely quantify k, hourly averaged 10 m height wind speeds for each district were obtained from the website of Shanghai Meteorological Bureau (http://www.weather.com.cn) during the entire study and used to calculate monthly averaged wind speed for N_2O flux calculation. This avoids including effects from short-term extreme values. To help constrain our modeled k value and resulting N_2O flux, a group of synthetic k values is also generated from a frequently referenced conceptual model that takes river hydrology into account (Clough *et al.*, 2007):

$$k = (17.19w^{1/2}d^{-1/2} + 0.31\mu^2)(Sc/600)^{-1/2}, \tag{3}$$

where w and d are river water velocity (m s^{-1}) and river depth (m), respectively.

All statistical tests were performed using SPSS (Version 17.0, SPSS Inc., Chicago, IL, USA). All N_2O and ancillary data were tested for normality with the Kolmogorov–Smirnov goodness–of–fit procedure and log-transformed as necessary to meet the assumption of statistical analyses. If the data were log normally distributed, the population mean of $\exp(\mu + (\sigma/2))$ was computed, where μ and σ are the arithmetic mean of ln (variable) and the variance of ln (variable), respectively (Beaulieu *et al.*, 2008). A one-way ANOVA followed by Fisher's least significant difference test for pairwise comparison was used to determine significant differences for variables compared among rivers within different areas and months. Pearson correlation was used to examine the correlations among independent variables. Simple linear regression was used to detect relationships between N_2O saturation and other environmental parameters within different areas. In addition, for data collected from February 2010 to December 2010 that measured DIC, DOC, and SO_4^{2-}, a stepwise multiple linear regression was used to further explore the relationship between N_2O saturation and water chemistry. The criteria for inclusion were F to enter > 4 and F to remove < 3.95 (Harrison & Matson, 2003).

Estimate of annual N_2O emission

To calculate the annual N_2O emission, a spatial interpolation technique was employed. Averaged N_2O flux in each sampling site was used as input data for interpolation; The ArcGIS 9.2 implementation of Kriging method was employed to interpolate N_2O flux from each sampling site into the

entire administrative territory of Shanghai; the layer of river network was then extracted from the resultant contour map. The river network layer was further rasterized with 1 m^2 unit block, which resulted in 461884221 blocks. N_2O flux was identified in each blocks, and the annual N_2O emission of the river network was calculated as the sum of emission in each rasterized 1 m^2 block.

N inputs and predicted N$_2$O emission

Following the IPCC methodology, we predicted N_2O emission using default EF_{5-r} and $EF_{EFFLUENT}$ values:

$$N_2O \text{ emission} = N_{LEACH} \times EF_{5-r} + N_{EFFLUENT} \times EF_{EFFLUENT}, \quad (4)$$

where N_{LEACH} and $N_{EFFLUENT}$ are the total N leached from agricultural sources (Gg N yr^{-1}) and total N in sewage effluents released into the river network (Gg N yr^{-1}), respectively. We estimated N_{LEACH} by assuming that (i) all DIN (NH_4^+-N plus NO_3^--N in this study) in rural rivers are from agricultural sources; and (ii) leaching N load in a river is proportional to the agricultural land area in its catchment. Consequently, leaching N load in the CM rivers was estimated by using annual averaged NH_4^+ and NO_3^- concentrations (Table 1) and total river discharge (Rosamond et al., 2012); leaching N load for the rivers in other districts was estimated according to the ratio of their agricultural land area to CM's (Table S2). Our N_{LEACH} estimate is conservative because (i) minor parts of N load in CM rivers may still be attributed to other sources, and (ii) leaching N per area in CM, a predominant agricultural area, may be higher than that in other districts.

By the end of 2011, there were 52 WWTPs servicing a population of approximately 23 million people in Shanghai city area, with 49 of them located in urban and suburban areas. Most WWTPs use an extended aeration treatment system with activated sludge procedures. From 2009 to 2010, about 2.84×10^8 tonnes of treated sewage was discharged annually to the river network (Table S3). In addition, there is still a substantial amount of untreated industrial and domestic sewage being directly released to the river network (Table S3). We calculated N input from treated sewage by assuming that its DIN concentration met the National Drainage Standard, 20 mg N l^{-1}. This assumption is somehow validated by Beaulieu et al. (2010b), who measured that average NH_4^+-N and NO_3^--N concentrations in effluents from a WWTP using a similar treatment method were 17.2 mg l^{-1} and 2.9 mg l^{-1}, respectively. For N input from untreated sewage we used DIN concentration of 35.9 mg N l^{-1}, mean concentration in receiving sewage of the Bailonggang WWTP, the largest WWTP of Shanghai which treatment capability occupies about 30% of total waste water of Shanghai.

Results

Meteorological data and river chemistry

Monthly air temperature and water temperature, ranging from 1.9 to 34.7 °C and 3.9 to −32.8 °C, respec-

tively, exhibited a consistent seasonal pattern with the lowest temperature occurring in February and highest in August (Fig. 2a). Wind speed for each sampling site ranged from 0.85 to 3.25 m s^{-1} over the study period. On a monthly basis, wind speed was significantly higher in April, 2011 ($P < 0.01$), while it did not differ significantly among other months.

Dissolved oxygen (DO) concentrations were generally under-saturated (Fig. 2b), ranging from 2.84 to 6.14 mg l^{-1} among districts (Table 1), and were positively related to the percentage of agricultural lands ($R^2 = 0.78$, $P < 0.05$). District-averaged NH_4^+-N concentrations showed significant variation, ranging from 1.25 to 5.40 mg l^{-1} (Table 1), and were generally highest in SP and BS ($P < 0.01$ in both cases) and lowest in CM ($P < 0.01$). Monthly averaged NH_4^+-N concentration in February 2011 was the highest among all months ($P < 0.01$ for all comparisons). A positive correlation was observed between the district-averaged NH_4^+-N and the percentage of urban land use ($R^2 = 0.68$,
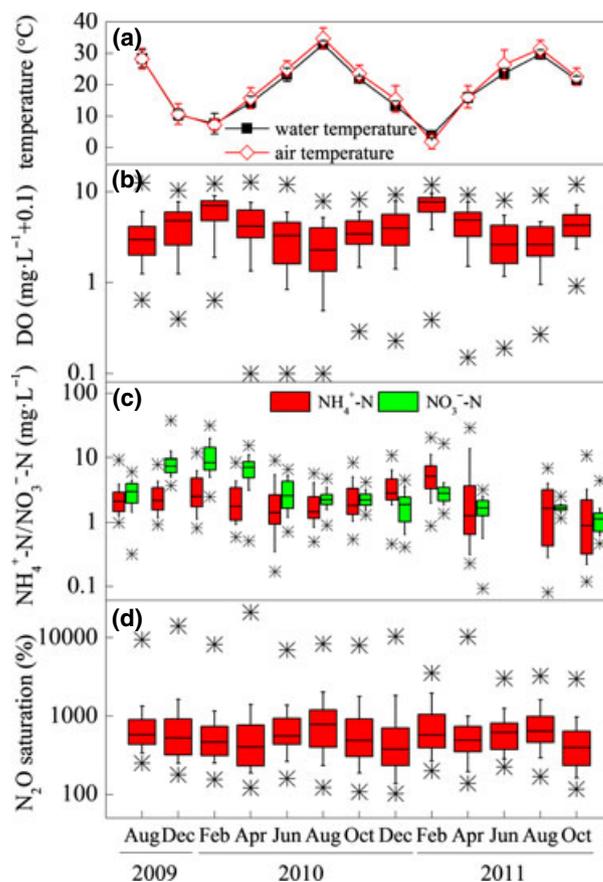
Fig. 2 Temporal variances of (a) DO, (b) NH_4^+-N, (c) NO_3^--N, and (d) N_2O saturation. The box extent, line inside the box, and error bars denote the 25th and 75th, 50th, 10th and 90th percentiles. Asterisks denote maximum and minimum value.

$P < 0.05$), while a negative correlation was observed between the monthly averaged NH_4^+-N and the water temperature ($R^2 = 0.72$, $P < 0.01$, Fig. 2c). With the exclusion of CM, NO_3^--N concentrations were less variable among districts, ranging from 3.27 to 4.78 mg l^{-1} (Table 1) and were positively related to agricultural lands ($R^2 = 0.69$, $P < 0.05$). It is worth noting that CM, with the highest agricultural land coverage, had the lowest NO_3^--N concentration (1.69 mg l^{-1}). Monthly averaged NO_3^--N concentration in February 2010 was the highest among all months ($P < 0.01$ for all comparisons). Water pH, salinity, DIC, DOC, and SO_4^{2-} concentrations did not have significant spatio-temporal variance over the study period (Table 1).

N_2O saturation and flux

Dissolved N_2O was supersaturated with respect to the atmosphere in all sample sites, on average ranging from 521 to 1073% between months (Fig. 2d). The overall mean N_2O saturation including all sampling sites for the entire study period was 770%.

N_2O saturation in August 2010 was significantly higher than in April 2011, June 2011, and October 2011; N_2O saturation in October 2011 was significantly lower than in December 2009 and April 2010 (Fig. 2d). But monthly averaged N_2O saturation had no significant correlation with ambient temperatures, wind speed, substrates, or atmospheric N_2O concentrations. Nevertheless, when N_2O saturation of December 2009 and February 2011 were not included, monthly averaged N_2O saturations showed a positive correlation with water temperature ($R^2 = 0.68$, $P < 0.05$). N_2O saturation was significantly different among three land use areas ($P < 0.01$ for all comparisons), with urban rivers having an average of up to 2500%, while saturation of rural rivers was lowest but still oversaturated.

When using all measured N_2O saturation data points, the simple linear regressions demonstrated a positive link between N_2O saturation and NO_3^--N concentration for urban and rural rivers (Fig. 4c), while N_2O saturation was negatively and positively related to DO and NH_4^+-N concentrations, respectively, for urban, suburban, and rural rivers (Fig. 4a and b). Multiple linear regressions show that the multi-predictor models are able to resolve 49%, 53%, 58%, and 59% of N_2O variance for urban, suburban, rural, and all rivers, respectively (Fig. 5). NH_4^+-N and water temperature are included in all regression models.

In this study, site-averaged k values used for flux calculation ranged from 3.1 cm h^{-1} to 6.0 cm h^{-1}. Four synthetic data sets were generated using annually averaged water temperature (18.9 °C), same wind speed range (0.85 to 3.25 m s^{-1}), typical river depths (0.5 to 10 m) and water flow velocity (0.1 m s^{-1}, 0.4 m s^{-1}, 0.7 m s^{-1}, 1 m s^{-1}) of the Shanghai river network. Our k values are significantly lower than synthetic k values under water flow velocity greater than 0.1 m s^{-1} ($P < 0.01$ in all comparisons) (Fig. 6). By using k values from Eqn (2) monthly averaged N_2O fluxes ranged from 1.10 to 2.71 mg N_2O-N m^{-2} d^{-1} with an overall mean of 1.91 mg N_2O-N m^{-2} d^{-1}. N_2O fluxes in the urban rivers (0.13 ± 0.05 to 52.10 ± 10.12 mg N_2O-N m^{-2} d^{-1}) were significant higher than those in suburban (0.04 ± 0.09 to 37.92 mg N_2O-N m^{-2} d^{-1}) and rural rivers (0.01 ± 0.01 to 8.62 ± 5.91 mg N_2O-N m^{-2} d^{-1}) ($P < 0.01$ in all comparisons).

Annual N_2O emission and emission predicted by IPCC

We calculated the annual N_2O emission of 0.29 Gg N_2O-N yr^{-1} from the whole river network by using Kriging interpolation. The leaching N and sewage N inputs were 36.00 Gg N yr^{-1} and 26.57 Gg N yr^{-1}, respectively (Table S2 and S3). Using default IPCC EF_{5-r} and $EF_{EFFLUENT}$ values, N_2O emission predicted from leaching and sewage N inputs was 0.22 Gg N_2O-N yr^{-1}, or about 76% of the measured annual emission.

Discussion

Spatio-temporal variability in N_2O saturation and its potential control

In this study, annually averaged N_2O saturation exceeded 400% in 70 out of 87 sites in the Shanghai river network, while comparably high N_2O concentrations have been reported from other eutrophic urban rivers and rivers impacted by urban sewage (Table S1). Temperature has been observed to affect N_2O production in some aquatic systems. In a large and impounded river Beaulieu *et al.* (2010b) found that water temperature positively correlated to N_2O saturation and explained 70% of the seasonal variance of N_2O saturation alone due to its stimulation on microbial N_2O production (Harrison & Matson, 2003). In parallel, seasonal changes in N_2O may also be controlled by changes of N loadings and availability of carbon in river water (Outram & Hiscock, 2012). More importantly, as summarized by Beaulieu *et al.* (2010b), the covariance among N availability and temperature can result in complex temporal patterns in N_2O saturation. Using water temperature as a proxy variable for seasonality, N_2O saturation did not exhibit a pronounced seasonality in our study. Nevertheless, NH_4^+ concentration was correlated negatively to water temperature over months, and the highest NH_4^+ and NO_3^- concentrations were
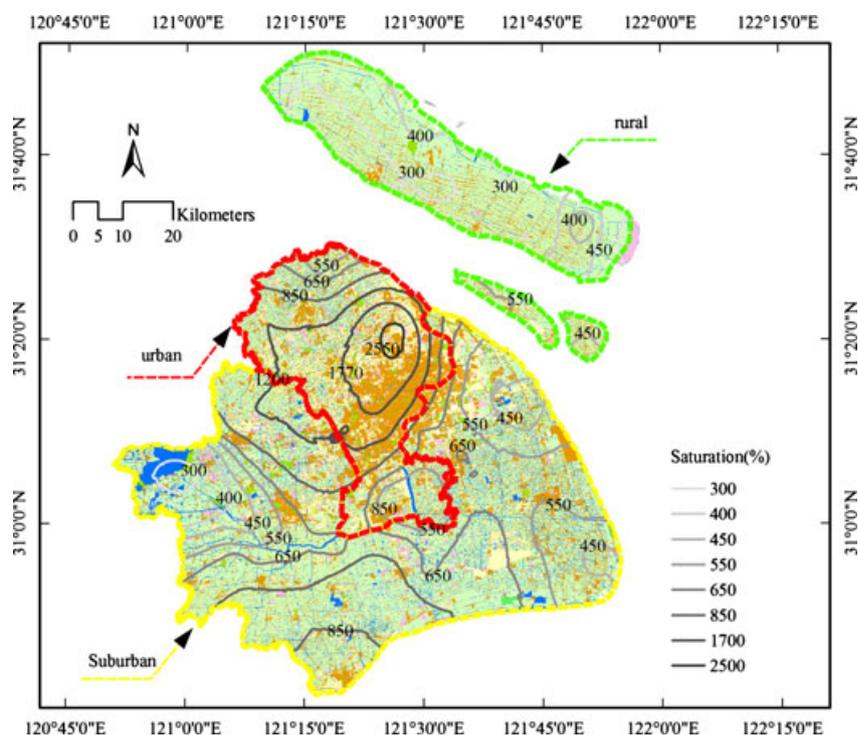
Fig. 3 Spatial characteristics of N$_2$O saturation with the overlap of land use.

found in the cold seasons (Fig. 2c). Monthly averaged N$_2$O saturation in turn correlated with water temperature positively when N$_2$O saturation from two winter surveys was excluded. Therefore, we suggested that temporal pattern of N$_2$O saturation in the Shanghai river network was regulated by the inverse tendencies between temperature and substrate delivery over the study period. While N$_2$O production was stimulated in the warm seasons, N$_2$O maintained super-saturation during the cold seasons due to the high substrate loadings. However, the observed seasonality of N substrate loadings in river water is not readily explainable. Unlike completely agricultural or other natural watersheds where N delivery to rivers could be linked to seasonal activities, for example, fertilization/irrigation, precipitation, water discharge, and groundwater supply (Outram & Hiscock, 2012), the Shanghai river network is subject to more complex N sources, some of which may be highly regulated by human activities and then seasonally unpredictable (e.g., sewage release, urban storm runoff, desilting, dam construction, and regulation). In particular, it is likely that frequent sewer flushing in winter seasons are responsible for the higher N substrate loadings in the river network. An N input budget with high temporal resolution of N substrates is the key to advance our understanding of N$_2$O seasonality.

In our study, higher N$_2$O saturation and N substrates were observed in urban and suburban rivers (Table 1; Fig. 3). This dependency between land use, N loadings, and N$_2$O is consistent with previous studies (e.g. Beaulieu *et al.*, 2010a; Rosamond *et al.*, 2012) but is revealed more clearly by our intensive sampling (Fig. 3). Interestingly, rural rivers had consistently lower NO$_3^-$ concentrations relative to urban and suburban rivers (Table 1), indicating that there might be other NO$_3^-$ sources rather than agriculture for urban and suburban rivers (e.g., sewage and/or NO$_3^-$ from active nitrification). N$_2$O saturation and NO$_3^-$ concentration were significantly correlated in urban and rural rivers (Fig. 4c), but overall NO$_3^-$ could only explain little variation in N$_2$O saturation, casting doubt on the generally accepted relationship between NO$_3^-$ and N$_2$O production rate frequently observed in agricultural rivers (Baulch *et al.*, 2011) and single large rivers (Yan *et al.*, 2012). On the other hand, NH$_4^+$-N was significantly and positively correlated with N$_2$O, explaining 18%, 14%, and 21% variability in N$_2$O saturations in urban, suburban, and all sampled rivers, respectively (Fig. 4b). This may suggest a significant nitrification source of N$_2$O, particularly in urban and suburban rivers. If N$_2$O was primarily produced via rapid nitrification process, we would expect to see a significant positive relationship between DO and N$_2$O in rivers with relatively high
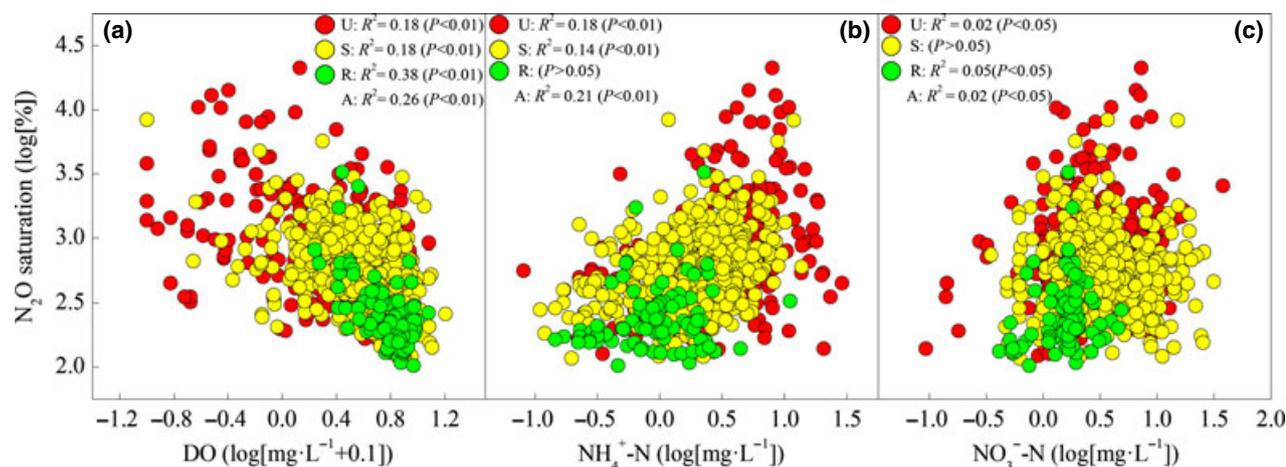
Fig. 4 Simple linear regression analysis of normalized N_2O saturation with (a) normalized DO, (b) normalized NH_4^+-N, and (c) normalized NO_3^--N for urban, suburban, and rural rivers. Each N_2O saturation data point is calculated from three independent replicates. Letter 'U', 'S', 'R', and 'A' in the figure represent urban, suburban, rural, and all rivers, respectively. Linear regression R^2 and P values are shown.

concentrations of NH_4^+-N (Harrison & Matson, 2003). In fact, however, DO was negatively correlated with N_2O saturation in the Shanghai river network and resolved more variances than NH_4^+ and NO_3^- as a single predictor (Fig. 4a). Moreover, in the stepwise multiple regressions that include DIC, DOC, and SO_4^{2-}, NH_4^+ or DO still stand out as a clearly superior predictor of N_2O saturation in urban and suburban rivers (Fig. 5). Since water temperature negatively relates to the solubility of oxygen in river water under natural conditions (Baulch *et al.*, 2012), the multiple regression also indicates that N_2O saturation in rural rivers and then in all sampled rivers were favored under a low DO, relatively low pH (7.4–7.6), and high NH_4^+ condition. Thus, these results may essentially indicate the inconsistency between the specific condition favoring great N_2O yielding in the Shanghai river network and those theoretically optimal for general nitrification or denitrification (Garnier *et al.*, 2009).

According to the 'hole in the pipe' model that compares N_2O production to water leakage from a pipe with holes (Baulch *et al.*, 2012), N_2O is released based on both the rate of N transformation processes (size of pipe) and the N_2O yield for these processes (size of hole in the pipe). In N-limited large rivers and estuaries, DO was found to positively correlate to N_2O produced from coupled nitrification-denitrification (Yan *et al.*, 2012). In contrast, in N-enriched estuaries and rivers, nitrification in sediments and the water column can be a net source of N_2O (Toyoda *et al.*, 2009), and both N_2O production rate and the N_2O yield from nitrification have been found to increase with decreasing aerobicity due primarily to incomplete aerobic nitrification (Kester
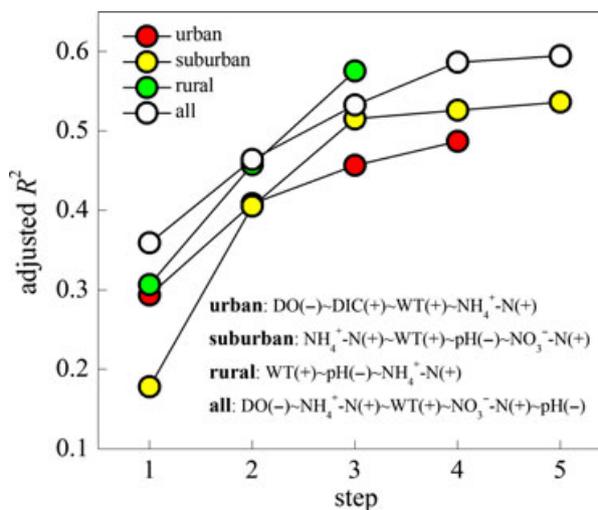
Fig. 5 Stepwise multiple regression analysis with log-transformed N_2O saturation as the dependent variable. Chosen data are from February 2010 to December 2010. Log normally distributed candidates are log-transformed before entered into the models. For each model, final set of predictors is shown in sequence. '+' and '−' in the brackets denote positive and negative relationships between predictor and N_2O saturation, respectively.

et al., 1997; Cébron *et al.*, 2005). In parallel, nitrifier-denitrification, a pathway of nitrification in which NH_4^+ is oxidized to NO_2^- followed by the reduction of NO_2^- to N_2O and N_2, can also account for the N_2O production under high NH_4^+ loading associated with low DO (Toyoda *et al.*, 2009). Several studies have confirmed that nitrifying bacteria possess an alternative

metabolism of denitrification in oxygen-depleted environments, and the reduction of NO_2^- with NH_4^+ as electron donor in this pathway is not as sensitive as denitrification to the aerobic condition (Shaw *et al.*, 2006). In the lower Seine River and estuary, nitrification and nitrifier-denitrification were found to be the dominant N_2O source and kinetically favorable under the optimal condition with DO concentration ranging from 1.1 to 1.5 mg O_2 l^{-1} (Cébron *et al.*, 2005). In our study, urban and suburban rivers suffer from high sewage input from WWTPs (Table S3). Urban sewage can be a major source of NH_4^+ and organic substances to the river network (Beaulieu *et al.*, 2008), causing severe NH_4^+ pollution and hypoxia in river water, which favors high N_2O production and N_2O yield from either aerobic nitrification or nitrifier-denitrification. It has also been reported that poorly nitrified WWTP effluents could stimulate N_2O production in both river water column and sediments by delivering nitrifying bacteria to receiving rivers (Beaulieu *et al.*, 2010b).

On the other hand, although the correlation between NO_3^--N and N_2O was weak in our study, denitrification as a source of N_2O cannot be totally ruled out. It is well known that even in a fully oxic water column, oxygen can be rapidly depleted in benthic sediments. The low DO and high NO_3^- concentrations observed in the Shanghai river network could indicate that denitrification rate might not be NO_3^--limited but actually be DO-dependent (Rosamond *et al.*, 2012). It has been shown that N_2O production by denitrification was maximal when the oxygen availability is very low, but not zero as the inhibition of N_2O reductase by O_2 is stronger than the inhibition of the other reductases of denitrification (Otte *et al.*, 1996). In this case, low oxygen penetration from the water column might create an aerobic–anaerobic interface closer to the sediment surface and subsequently facilitate more diffusion of denitrification-derived N_2O to the overlying water.

In summary, this study reveals the controls of NH_4^+ and DO on N_2O production in Shanghai river network by creating a suboptimal condition, favoring high N_2O yields, for both nitrifiers and denitrifiers. While nitrification and denitrification were stimulated by high N loadings and then set the boundaries of the possible N_2O production, in the Shanghai river network the water hypoxia, controlled by urban sewage release, may largely affect the extent to which these processes produce N_2O as a by-product and to which produced N_2O can diffuse into river water (Rosamond *et al.*, 2012). Generally, DO might exert more effects in the Shanghai river network than in other less managed systems because of the higher observed NH_4^+ and NO_3^- loadings in urban and suburban rivers. Riverine

N_2O concentrations or emissions are subject to a pronounced diel cycle with decreased DO and pH in river water at night (Baulch *et al.*, 2012). While we did not sample during night-time in this study, from the observed relationships (Fig. 5) increased water hypoxia and decreased pH at night may have played an important role in keeping N_2O supersaturated in the Shanghai river network.

Annual N_2O emission and its implication for IPCC method

It has been shown that in shallow streams and rivers the source of turbulence in the surface aqueous boundary layer can originate from both wind and water-shear produced turbulence, and k depends on the depth, flow velocity, and wind regime of a given river (Raymond & Cole, 2001). As shown in Figure 6 our k-values estimated from a wind-dependent model are generally lower than synthetic values from the model taking river hydrology into account. Given that the majority of sampled rivers had a depth shallower than 10 m and wind speed in the city is low, bottom stress caused by water flow might dominate the turbulence (Raymond & Cole, 2001), and thus our estimated N_2O emissions might be highly underestimated particularly when the river water flow was accelerated by tidal motion. Future efforts, particularly tracer studies and investigations on river hydraulic geometry (Raymond *et al.*, 2012), are
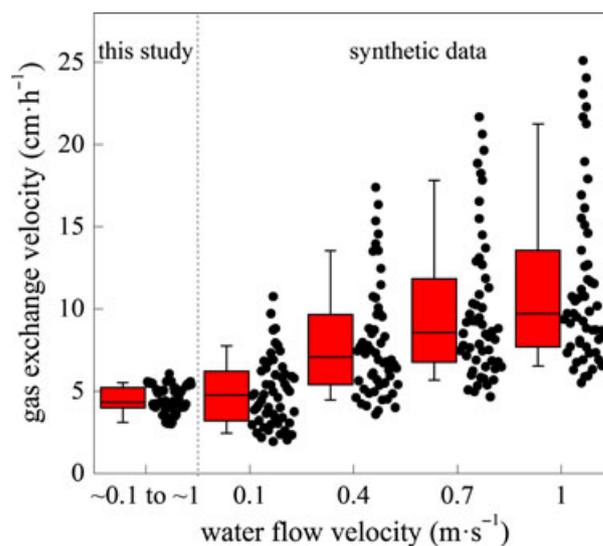
Fig. 6 Comparison between modeled gas exchange velocities used in this study and synthetic data generated from Eqn (3). The box extent, line inside the box, and error bars denote the 25th and 75th, 50th, 10th and 90th percentiles of the data set.

needed to precisely quantify the dynamics of k. Moreover, how to scale measured k values across this large, tidal-influenced river system with a reasonable temporal resolution must be appropriately solved for improving large scale N_2O emission estimates (Raymond *et al.*, 2012).

Regardless of the potential underestimation, N_2O fluxes in the Shanghai river network are among the highest values reported from river systems (Table S1). Beaulieu *et al.* (2008) concluded that N_2O emission rates exceeding 12 mg N_2O-N m^{-2} d^{-1} are spatially limited and linked to a N_2O point source. In our studies, N_2O flux as high as 31 mg N_2O-N m^{-2} d^{-1} was observed in one urban river of BS, but only one urban river had an annual mean N_2O emission rates exceeding 12 mg N_2O-N m^{-2} d^{-1}. Our long-term observation, which accounts for considerable temporal variability of N_2O emission rates might be more representative to demonstrate N_2O emissions from urban rivers compared to other short-term or seasonal studies. When compared to another long-term study (29 months) by Baulch *et al.* (2011) in five Canadian streams draining multiple land use, N_2O emissions from Shanghai river network were generally higher than their annual emission estimates (-0.09 to 1.53 mg N_2O-N m^{-2} d^{-1}). Our measured N_2O emissions were also substantially higher than seasonal mean emission from the main stem of Yangtze River, ranging from 0.04 to 0.96 mg N_2O-N m^{-2} d^{-1} (Yan *et al.*, 2012), annual mean emission from Yangtze River estuary (Zhang *et al.*, 2010), ranging from 0.22 to 0.48 mg N_2O-N m^{-2} d^{-1}, and from its adjacent estuarine wetland, up to 2.36 mg N_2O-N m^{-2} d^{-1} in summertime (Yu *et al.*, 2012), which receiving nutrient loadings exported by Yangtze River, are considered as hotspot of N_2O emission within this large river basin.

Based on ^{15}N tracer experiments and implementation of Global NEWS model, Beaulieu *et al.* (2010a) estimated that at global scale N_2O emission from aquatic system is 0.68 Tg N_2O-N yr^{-1}, which yields a global emission density, calculated as the annual N_2O emission per water surface area, of 242 mg N_2O-N m^{-2} yr^{-1} (global benthic surface area was presented by Wollheim *et al.* (2008)). With the surface water area of Shanghai river network to be 569.6 km^2, calculated emission density is 492 mg N_2O-N m^{-2} yr^{-1}, two times higher than global average but in accordance with the range of 356–707 mg N_2O-N m^{-2} yr^{-1} reported from Seine river network draining through a huge metropolitan area (Garnier *et al.*, 2009). Based on our investigation, sewage N input accounted for about 43% of the total DIN input to the Shanghai river network, while current results from N cycling models showed that sewage N input was the smallest contributor to the total DIN input in contemporary era, accounting for about 4% in Yangtze River basin (Yan *et al.*, 2010) and 7% at global scale (Seitzinger & Kroeze, 1998). Some studies suggested that sewage effluents function as a large N_2O point source to river water, directly enhancing riverine N_2O emissions (Hemond & Duran, 1989). However, by assuming typical values, 16.7–46.0 μg N_2O-N l^{-1} (Hemond & Duran, 1989; Beaulieu *et al.*, 2010b), for dissolved N_2O concentration in sewage effluent, direct N_2O input from WWTPs effluents was 0.005–0.013 Gg N_2O-N yr^{-1} or 1.7–4.5% of measured annual emission. Since DIN is rapidly consumed and recycled in river systems, our study provides a critical indication that urban sewage may be disproportionately important for small urban rivers primarily in terms of its stimulation on microbial N_2O production.
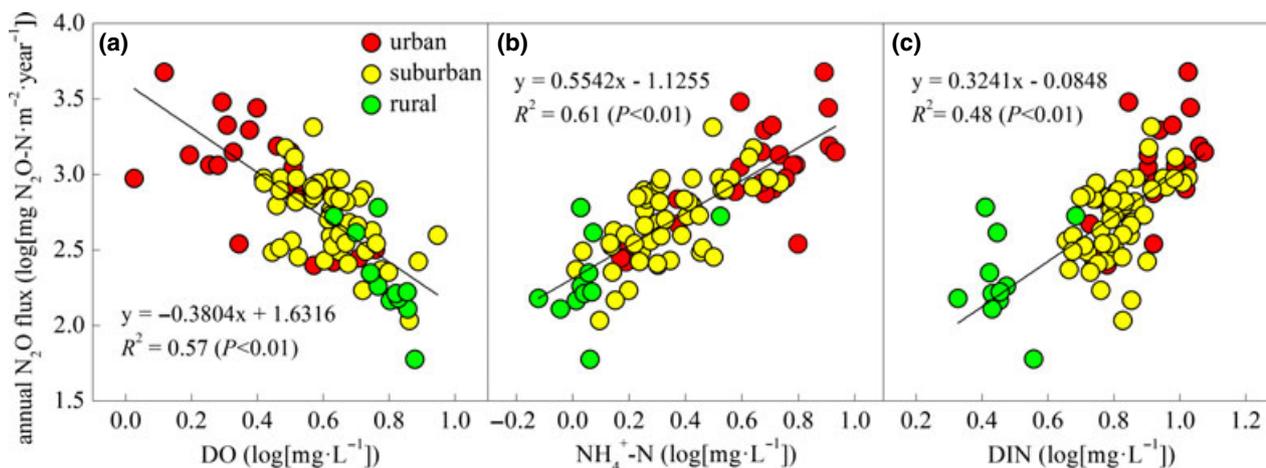
Fig. 7 Relationship between (a) annual average DO, (b) NH_4^+-N, dissolved inorganic nitrogen (DIN) and (c) N_2O flux from urban, suburban, and rural rivers. Linear regressions shown in the figure are based on all data from three areas.

Using IPCC method, predicted N_2O emission underestimates annual N_2O emission by 24%. We argue that the current method needs to be refined to re-evaluate the role of urban rivers in the global budget. Specifically, the role of nitrification and its N_2O yielding should be reconsidered for urban rivers. Now it is somewhat clear that factors controlling N_2O emission are very different between agricultural rivers and rivers impacted by urban activities (Table S1). In the Shanghai river network, both NH_4^+ and DO concentrations are better predictors of site-averaged N_2O flux than DIN (Fig. 7), highlighting those factors influencing nitrification rate and its N_2O yielding are key to understand and predict N_2O production and emission in urban watersheds. However, although IPCC method assumes nitrification rate in rivers exceeding denitrification by twofold, to our knowledge, there are few field measurements performed in urban rivers to validate this value. In pure culture, Kester et al. (1997) incubated the nitrifier Nitrosomonas europaea at different oxygen saturations and found that 0.15% of NH_4^+ was converted into N_2O at 80% oxygen saturation, and 0.8% at 1% saturation. A recent study by Rosamond et al. (2012) also emphasized the nonlinear relationship between DIN input and N_2O emissions and the superior role of DO in predicting N_2O in a sewage-impacted river. As supported by other studies conducted in urban-impacted rivers, in which NH_4^+ or DO was frequently reported to control N_2O emissions (Table S1), the controls of NH_4^+ and DO on N_2O emissions in urban rivers may thus have global importance that requires future efforts to integrate these controls into global riverine N_2O budget.

Acknowledgements

References

Baulch HM, Schiff SL, Maranger R, Dillon PJ (2011) Nitrogen enrichment and the emission of nitrous oxide from streams. Global Biogeochemical Cycles, 25, GB4013.

Baulch HM, Dillon PJ, Maranger R, Venkiteswaran JJ (2012) Night and day: short-term variation in nitrogen chemistry and nitrous oxide emissions from streams. Freshwater Biology, 57, 509–525.

Beaulieu JJ, Arango CP, Hamiltion SK, Tank JL (2008) The production and emission of nitrous oxide from headwater streams in the Midwestern United States. Global Change Biology, 14, 878–894.

Beaulieu JJ, Tank JL, Hamilton SK et al. (2010a) Nitrous oxide emission from denitrification in stream and river networks. PNAS, 108, 214–219.

Beaulieu JJ, Shuster WD, Rebholz JA (2010b) Nitrous oxide emissions from a large, impounded river: the Ohio River. Environmental Science and Technology, 44, 7527–7533.

Cébron A, Garnier J, Billen G (2005) Nitrous oxide production and nitrification kinetics by natural bacterial communities of the lower Seine river (France). Aquatic Microbial Ecology, 41, 25–38.

Clough TJ, Buckthought LE, Kelliher FM, Sherlock RR (2007) Diurnal fluctuations of dissolved nitrous oxide concentrations and estimates of N_2O emissions from a spring-fed river implications for IPCC methodology. Global Change Biology, 13, 1016–1027.

Davidson EA (2009) The contribution of manure and fertilizer nitrogen to atmospheric nitrous oxide since 1860. Nature Geosciences, 2, 659–662.

De Klein C, Novoa RSA, Ogle S et al. (2006) Chapter 11: N_2O emissions from managed soils, and CO_2 emissions from lime and urea application. In: Vol 4—Agriculture, Forestry and Other Land Use, 2006 IPCC Guidelines for National Greenhouse Gas Inventories, (eds Eggleston S, Buendia L, Miwa K, Ngara T, Tanabe K), pp. 11.1–11.54. Institute for Global Environmental Strategies, Japan.

Doorn MRJ, Towprayoon S, Vieira SMM et al. (2006) Chapter 6: Wastewater treatment and discharge. In: Vol 5—Waste, 2006 IPCC Guidelines for National Greenhouse Gas Inventories, (eds Eggleston S, Buendia L, Miwa K, Ngara T, Tanabe K), pp. 6.1–6.21. Institute for Global Environmental Strategies, Japan.

Garnier J, Billen G, Vilain G, Martinez A, Silvestre M, Mounier E, Toche F (2009) Nitrous oxide (N_2O) in the Seine river and basin: observations and budgets. Agriculture, Ecosystems and Environment, 133, 223–233.

Harrison J, Matson P (2003) Patterns and controls of nitrous oxide emissions from waters draining a subtropical agricultural valley. Global Biogeochemical Cycles, 17, 1080.

Hemond HF, Duran AP (1989) Fluxes of N_2O at the sediment-water and water-atmosphere boundaries of a nitrogen-rich river. Water Resources Research, 25, 839–846.

Ivens WPMF, Tysmans DJJ, Kroeze C, Löhr AJ, van Wijnen J (2011) Modeling global N_2O emissions from aquatic systems. Current Opinion in Environmental Sustainability, 3, 350–358.

Kester RA, De Boer W, Laanbroek HJ (1997) Production of NO and N_2O by pure cultures of nitrifying and denitrifying bacteria during changes in aeration. Applied and Environmental Microbiology, 63, 3872–3877.

Otte S, Grobben NG, Robertson LA, Jetten MS, Kuenen JG (1996) Nitrous oxide production by Alcaligenes faecalis under transient and dynamic aerobic and anaerobic conditions. Applied and Environmental Microbiology, 62, 2421–2426.

Outram FN, Hiscock KM (2012) Indirect nitrous oxide emissions from surface water bodies in a lowland arable catchment: a significant contribution to agricultural greenhouse gas budgets? Environmental Science and Technology, 46, 8156–8163.

Ravishankara AR, Daniel JS, Portmann RW (2009) Nitrous oxide (N_2O): the dominant ozone-depleting substance emitted in the 21st century. Science, 326, 123–125.

Raymond PA, Cole JJ (2001) Gas exchange in rivers and estuaries: choosing a gas transfer velocity. Estuaries, 24, 312–317.

Raymond PA, Zappa CJ, Butman D, Bott TL et al. (2012) Scaling the gas transfer velocity and hydraulic geometry in streams and small rivers. Limnology & Oceanography: Fluids & Environments, 2, 41–53.

Rosamond MS, Thuss SJ, Schiff SL (2012) Dependence of riverine nitrous oxide emissions on dissolved oxygen levels. Nature Geosciences, 5, 715–718.

Seitzinger SP, Kroeze C (1998) Global distribution of nitrous oxide production and N inputs in freshwater and coastal marine ecosystems. Global Biogeochemical Cycles, 12, 93–113.

Seto KC, Güneralp B, Hutyra LR (2012) Global forecasts of urban expansion to 2030 and direct impacts on biodiversity and carbon pools. PNAS, 109, 16083–16088.

Shanghai Water Bureau (2011) Available at: http://www.shanghaiwater.gov.cn/swEng/index.jsp (accessed 10 February 2012).

Shaw LJ, Nicol GW, Smith Z, Fear J, Prosser JI, Baggs EM (2006) Nitrosospira spp. can produce nitrous oxide via a nitrifier denitrification pathway. Environmental Microbiology, 8, 214–222.

Toyoda S, Iwai H, Koba K, Yoshida N (2009) Isotopomeric analysis of N_2O dissolved in a river in the Tokyo metropolitan area. Rapid Communications in Mass Spectrometry, 23, 809–821.

Van Drecht G, Bouwman AF, Harrison J, Knoop JM (2009) Global nitrogen and phosphate in urban wastewater for the period 1970 to 2050. Global Biogeochemical Cycles, 23, GB0A03.

Wang D, Chen Z, Sun W, Hu B, Xu S (2009) Methane and nitrous oxide concentration and emission flux of Yangtze Delta plain river net. Science in China Series B: Chemistry, 52, 652–661.

Weiss RF, Price BA (1980) Nitrous oxide solubility in water and seawater. *Marine Chemistry*, **8**, 347–359.

Wollheim WM, Vörösmarty CJ, Bouwman AF *et al.* (2008) Global N removal by freshwater aquatic systems using a spatially distributed, within-basin approach. *Global Biogeochemical Cycles*, **22**, GB2026.

Xu S, Shu J, Wang Z *et al.* (2004) *Atlas of Shanghai Urban Physical Geography.* China Map Press, Shanghai.

Yan W, Mayorga E, Li X, Seitzinger S, Bouwman AF (2010) Increasing anthropogenic nitrogen inputs and riverine DIN exports from the Changjiang River basin under changing human pressures. *Global Biogeochemical cycles*, **24**, GB0A06.

Yan W, Yang L, Wang F, Wang J, Ma P (2012) Riverine N_2O concentrations, exports to estuary and emissions to atmosphere from the Changjing River in response to increasing nitrogen loads. *Global Biogeochemical cycles*, **26**, GB4006, doi: 10.1029/2010GB003984.

Yu Z, Li Y, Deng H, Wang D, Chen Z, Xu S (2012) Effect of Scirpus mariqueter on nitrous oxide emissions from a subtropical monsoon estuarine wetland. *Journal of Geophysical Research*, **117**, G02017.

Zhang GL, Zhang J, Liu SM, Ren JL, Zhao YC (2010) Nitrous oxide in the Changjiang Estuary and its adjacent marine area riverine input sediment release and atmospheric fluxes. *Biogeosciences*, **7**, 3505–3516.